Numerical investigation of a methane/air triple flame

Guo, Hongsheng; Liu, Fengshan; Smallwood, Gregory

Publisher's version / Version de l'éditeur:

The 3rd International Conference on Computational Heat and Mass Transfer [Proceedings], pp. 1-10, 2003

NRC Publications Archive Record / Notice des Archives des publications du CNRC :
https://nrc-publications.canada.ca/eng/view/object/?id=f209a6b8-9a7b-49e7-8f78-fc1d6a4f90c0
https://publications-cnrc.canada.ca/fra/voir/objet/?id=f209a6b8-9a7b-49e7-8f78-fc1d6a4f90c0

Proceedings of 3ICCHMT
3rd International Conference on Computational Heat and Mass Transfer
May 26-30, 2003, Banff, CANADA
Paper Number "32"

NUMERICAL INVESTIGATION OF A METHANE/AIR TRIPLE FLAME

Hongsheng Guo, Fengshan Liu, and Gregory J. Smallwood
Combustion Research Group
National Research Council of Canada
1200 Montreal Road, Ottawa, Ontario K1A 0R6
hongsheng.guo@nrc.ca

ABSTRACT

The flame in a methane/air mixing layer was investigated by numerical simulation. The primitive variable method, in which the fully elliptic governing equations were solved with detailed chemistry and complex thermal and transport properties, was used. Radiation heat transfer from CO_2, CO and H_2O was calculated using the discrete-ordinates method coupled to a SNBCK based wide band model.

The results indicate that the structure that evolves in a laminar methane/air mixing layer is a triple flame, which consists of a diffusion flame and two premixed flames. The heat release rate in the diffusion flame is much lower than in the premixed flames. No primary fuel can reach the diffusion flame, while excess oxygen can survive through the lean premixed flame and diffuse to the diffusion flame. The temperature in the diffusion flame is higher than in the premixed flames. As a whole, the triple flame propagation speed is higher than the planar laminar flame speed of a stoichiometric methane/air mixture, primarily due to the flow field divergence ahead the triple region.

INTRODUCTION

In many important applications, such as in a direct injection spark-ignited (DISI) engine, combustion occurs under partially premixed and stratified conditions. In a partially premixed mixture field a flame propagates preferentially along the stoichiometric surface. At the leading edge of this propagating flame, a two-dimensional structure is observed that consists of a diffusion flame embedded within a fuel-lean and a fuel-rich premixed flame. These flames are called triple flames. The region where the three flames meet is called the triple region.

The triple flame phenomenon was first observed by Phillips [1] in 1965 in an experimental study of a methane/air mixing layer. The problem was later addressed by Liñán and Crespo [2] using large activation energy asymptotics in 1976. In 1989, this analytical approach was extended by Dold [3] to include the upstream heat conduction. Using a similar model, Kĩoni et al. [4] studied the response of the structure and propagation velocity of a triple flame to the strain in a counterflow configuration by a simplified numerical model. Then the issue was revisited by some researchers from different viewpoints. The effect of heat release on triple flame was studied by Ruetsch et al. [5] by a simplified numerical scheme and a one-step chemistry model. Echekki and Chen [6] calculated the structure and propagation of a methanol-air triple flame by detailed chemistry. Azzoni et al. [7] studied the gravity effects on triple flames. Plessing et al. [8] experimentally and numerically studied the structure of a triple flame produced by an axisymmetric co-flow burner with a central diluted fuel jet and a surrounding fuel co-flow. Qin et

al. [9] also studied the characteristics of lifted triple flame stabilized in the near field of a partially premixed axisymmetric jet. Kĩoni et al. [10] investigated the structure of a triple flame in a methane/air mixing layer experimentally and numerically by using a C1 chemistry scheme, with radiation heat transfer being neglected. Im and Chen [11, 12] studied triple flames in partially premixed hydrogen-air mixtures and the effects of flow strain on triple flame propagation by direct numerical simulation. Lockett et al. experimentally examined the structure and stability of the laminar counterflow triple flame [13].

In almost all the previous numerical studies on triple flame, certain simplifications have been used, such as the simplified chemistry, numerical scheme or neglecting of radiation heat loss from the flame. In the present paper, the triple flame in a methane/air mixing layer was numerically investigated while avoiding such simplifications. We employed the primitive variable method in which the fully elliptic governing equations were solved with detailed chemistry and complex thermal and transport properties. Radiation heat transfer from the flame was calculated using the discrete-ordinates method coupled to a SNBCK based wide band model. The governing equations and the numerical configuration will be described first in the following section, followed by the numerical results and discussions. Finally concluding remarks are given.

NUMERICAL CONFIGURATION AND MODEL

Figure 1 shows the computational flame configuration. The simulation was conducted in a two dimensional rectangular domain. The fresh methane/air mixture enters the domain from the bottom at 50 cm/s with the temperature of 298 K. The equivalence ratio at the inlet linearly varies from 0.0 to 2.0 within a 6-cm mixing layer. To avoid the effect of boundary locations on the numerical results, the computational domain was extended by 4 cm on each side of the mixing layer. The inlet equivalence ratios for the extended domain on each side of the mixing layer are 0.0 and 2.0, respectively. The total computational domain consists of a 14 x 30 cm^2 rectangular region. The free slip boundary condition was used for the left and right hand side boundaries, and zero gradient condition was used for the outlet.

The numerical model solved fully elliptic governing equations for the conservation of mass, momentum, energy and every chemical species. The governing equations are [14]:

Continuity:

$$\frac{\partial}{\partial x}(\rho u)+\frac{\partial}{\partial y}(\rho v)=0 \tag{1}$$

Momentum:

$$\rho u\frac{\partial u}{\partial x}+\rho v\frac{\partial u}{\partial y}=-\frac{\partial p}{\partial x}+2\frac{\partial}{\partial x}\left(\mu\frac{\partial u}{\partial x}\right)+\frac{\partial}{\partial y}\left(\mu\frac{\partial u}{\partial y}\right)$$
$$-\frac{2}{3}\frac{\partial}{\partial x}\left(\mu\frac{\partial u}{\partial x}\right)-\frac{2}{3}\frac{\partial}{\partial x}\left(\mu\frac{\partial v}{\partial y}\right)+\frac{\partial}{\partial y}\left(\mu\frac{\partial v}{\partial x}\right) \tag{2}$$

$$\rho u\frac{\partial v}{\partial x}+\rho v\frac{\partial v}{\partial y}=-\frac{\partial p}{\partial y}+2\frac{\partial}{\partial y}\left(\mu\frac{\partial v}{\partial y}\right)+\frac{\partial}{\partial x}\left(\mu\frac{\partial v}{\partial x}\right)$$
$$-\frac{2}{3}\frac{\partial}{\partial y}\left(\mu\frac{\partial u}{\partial x}\right)-\frac{2}{3}\frac{\partial}{\partial y}\left(\mu\frac{\partial v}{\partial y}\right)+\frac{\partial}{\partial x}\left(\mu\frac{\partial u}{\partial y}\right)-\rho g \tag{3}$$

Energy:

$$c_p\left(\rho u\frac{\partial T}{\partial x}+\rho v\frac{\partial T}{\partial y}\right)=\frac{\partial}{\partial x}\left(\lambda\frac{\partial T}{\partial x}\right)+\frac{\partial}{\partial y}\left(\lambda\frac{\partial T}{\partial y}\right)$$
$$-\sum_{k=1}^{KK}\left[\rho c_{pk}Y_k\left(V_{kx}\frac{\partial T}{\partial x}+V_{ky}\frac{\partial T}{\partial y}\right)\right]-\sum_{k=1}^{KK}h_kW_k\omega_k+q_r \qquad (4)$$

Gas species:

$$\rho u\frac{\partial Y_k}{\partial x}+\rho v\frac{\partial Y_k}{\partial y}=-\frac{\partial}{\partial x}\left(\rho Y_kV_{kx}\right)-\frac{\partial}{\partial y}\left(\rho Y_kV_{ky}\right)+W_k\omega_k\,,$$
$$k=1,\ 2,\ \ldots,\ KK \qquad (5)$$

where u and v are the velocities in x and y directions, respectively; T the temperature of the mixture; ρ the density of the mixture; W_k the molecular weight of the k^{th} species; λ the mixture thermal conductivity; c_p specific heat of the mixture under constant pressure; c_{pk} specific heat of the k^{th} species under constant pressure; ω_k mole production rate of the k^{th} species per unit volume. Quantity h_k denotes the specific enthalpy of the k^{th} species; g the gravitational acceleration; μ the viscosity of the mixture; Y_k the mass fraction of the k^{th} species; V_{kx} and V_{ky} the diffusion velocities of the k^{th} species in x and y directions; and KK the total species number.

The last term on the right hand side of Eq. 4, q_r, is the source term due to radiation heat transfer. It was obtained by the discrete ordinate method coupled to a statistical narrow-band correlated-K (SNBCK) based wide band model for the properties of CO, CO_2 and H_2O [15].

The species diffusion velocity consists of three terms: ordinary diffusion, thermal diffusion and correction diffusion velocities. Therefore:

$$V_{kx_i}=V_{okx_i}+V_{Tkx_i}+V_{cx_i}\,, \qquad k=1,2,\ldots,KK,\quad x_i=x,\ y \qquad (6)$$

The ordinary diffusion velocity V_{okx_i}, caused by concentration gradient, was obtained by the approximate mixture-average formulation, i.e.

$$V_{okx_i}=-\frac{1}{Y_k}D_k\frac{\partial Y_k}{\partial x_i}\,, \qquad k=1,2,\ldots,KK,\quad x_i=x,\ y \qquad (7)$$

Quantity V_{Tkx_i} is the thermal diffusion velocity, caused by temperature gradient, in x_i (x or y) direction for the k^{th} species. It was obtained by [16]:

$$V_{Tkx_i}=-\frac{D_k^T}{\rho Y_k}\frac{1}{T}\frac{\partial T}{\partial x_i}\,, \qquad k=1,2,\ldots,KK,\quad x_i=x,\ y \qquad (8)$$

where D_k^T is the multi-component thermal diffusion coefficient obtained by the method given by Kee et al. [16].

The correction diffusion velocity V_{cx_i} was introduced to ensure that the net diffusive flux of all species is zero.

Quantity D_k in Eq. 7 was related to the binary diffusion coefficients through the expression:

$$D_k = \frac{1 - X_k}{\sum_{j \neq k}^{KK} X_j / D_{jk}}, \qquad k=1,2,\ldots,KK \tag{9}$$

where X_k is the mole fraction of the k^{th} species, and D_{jk} is the binary diffusion coefficient.

The governing equations were discretized using the control volume method. The SIMPLE numerical scheme [17] was used to deal with the pressure and velocity coupling. The diffusion and convective terms in the conservation equations were respectively discretized by the central and upwind difference methods. The adaptive refinement of mesh was done, so that more meshes were put in the high temperature gradient region. The discretized equations of species mass fractions were solved in a fully coupled fashion on every grid to accelerate the convergence process [18], while those of momentum, energy and pressure correction were solved using the tri-diagonal matrix algorithm (TDMA).

The chemical reaction mechanism used is essentially from GRI-Mech 3.0 [19], with the removal of all the reactions and species related to NO_X formation. The revised reaction scheme consists of 36 species and 219 reactions. All the thermal and transport properties were obtained by using the database of GRI-Mech 3.0 and the algorithms given in [16, 20].

RESULTS AND DISCUSSIONS

To analyze the structure and characteristics of a triple flame, the parameter mixture fraction is used. It is defined as [21]:

$$\xi = \frac{\frac{2Z_C}{W_C} + \frac{Z_H}{2W_H} + \frac{\left(Z_{O,air} - Z_O\right)}{W_O}}{\frac{2Z_{C,fuel}}{W_C} + \frac{Z_{H,fuel}}{2W_H} + \frac{Z_{O,air}}{W_O}} \tag{10}$$

where Z_i denotes the mass fraction of the element i of atomic mass W_i, and the subscripts C, H and O refer to carbon, hydrogen and oxygen. The subscript *air* and *fuel* refer to the fuel and air stream reference states. In the present paper, these reference states are respectively the pure methane and air. The stoichiometric mixture fraction, ξ_s, of undiluted methane/air mixture is 0.0548. A dashed line in most figures of following sections indicates the position of the stoichiometric mixture fraction.

General structure of the flame

Figure 2 illustrates the distribution of the heat release rate. The structure of a triple flame is clearly shown. There are three main heat release regions. The left branch is formed due to the combustion of lean premixed mixture, while the right branch is due to the combustion of rich premixed mixture. Between the two premixed flames, there is a diffusion flame formed along the stoichiometric mixture fraction line. The three flames merge at the lower flame region, called triple region. The heat release rate in the diffusion flame is about two orders of magnitude smaller than in the premixed flames.

The concentrations of fuel (CH_4) and oxygen are shown in Fig. 3. It is found that almost no fuel can reach the stoichiometric line. Therefore most fuel is consumed in the premixed flames. On the rich side (right hand side), oxygen is entirely consumed by the premixed flame and cannot reach the diffusion

flame. However excess oxygen persists through the lean premixed flame, and diffuses toward and is subsequently consumed in the diffusion flame. Echekki and Chen [6] also observed this phenomenon in their simulation of a methanol-air triple flame.

In Fig. 4 the concentrations of H_2 and CO, two relatively stable intermediate species during methane combustion, are shown. It is illustrated that more H_2 and CO exist in the region between the rich premixed flame and diffusion flame. This is because there is not enough oxidant to convert the H_2 and CO, which are formed in the rich premixed flame, to H_2O and CO_2 in this region. These CO and H_2 are oxidized into CO_2 and H_2O in the diffusion flame.

The concentrations of three intermediate species, OH, O and H, are shown in Fig 5. It is indicated that the OH concentration peaks in the triple region. The concentration of OH in the diffusion flame is higher than in the premixed flames. For O radical, the concentration also peaks in the triple region, and the concentration in the lean premixed flame is higher than in diffusion and rich premixed flames. However, the concentration of H radical in the rich premixed flame is higher than in the diffusion and lean premixed flames.

Shown in Fig. 6 are the concentrations of two main products of methane combustion, H_2O and CO_2. It is noted that both concentrations peak in the diffusion flame. This is because the H_2O and CO_2 produced in the premixed flames are transported to the diffusion flame by convection and diffusion, and the CO and H_2 formed in the rich premixed flame are also oxidized to H_2O and CO_2 in the diffusion flame. However more H_2O exists on the rich side than on the lean side. The main formation reaction of CO_2 is $CO + OH = CO_2 + H$. For the formation of H_2O, although the reaction $H_2 + OH = H_2O + H$ is the most important one, the reactions $OH + CH_4 = H_2O + CH_3$ and $OH + CH_3 = CH_2(S) + H_2O$ also play significant roles.

The temperature distribution is shown in Fig. 7. It is indicated that temperature peaks around the stoichiometric line. Therefore there is heat transfer from the diffusion flame to the two premixed flames, due to conduction and radiation. This may cause the propagation speed and the flammability limit of the premixed flames to be different from those of the traditional lean or rich premixed flames.

Velocity field

Although the inlet velocity of the fresh mixture (50 cm/s) is higher than the planar laminar flame speed of a stoichiometric methane/air mixture (~40 cm/s [22]), the triple flame can be self-stabilized. To analyze the triple flame stabilization mechanism, the velocity field is examined below.

In Fig. 8, the streamlines are superimposed on the distribution of heat release to show the velocity field of the triple flame. It is found that the flow field diverges ahead of the triple region. This is caused by thermal expansion. The divergence of streamlines results in the decrease of the local flow speed ahead of the flame. Therefore the local velocity ahead of the flame is lower than the inlet velocity (50 cm/s).

Fig. 9 shows the flow speed along the stoichiometric line. It can be found that the velocity does decrease to a minimum value after the fresh mixture enters the domain, and then sharply increases. The velocity decrease is caused by the streamline divergence, and the increase by the temperature rise due to the heat release of combustion. The minimum speed along the stoichiometric line is indeed approximately the planar laminar flame speed of a stoichiometric methane/air mixture, which is about 40 cm/s [22].

Therefore it can be concluded that the reason that triple flame can be stabilized for an upstream flow speed higher than the planar laminar flame speed of a stoichiometric mixture is the divergence of streamlines ahead of the flame.

Local flame propagation speed

The local flame propagation speed along the front of the triple flame was obtained by evaluating the fluid velocity component normal to a flame contour. The flame propagation speed obtained by this method (S_L) depends on the selection of the iso-contour. To remove this effect, the obtained local flame propagation speed is converted to the density-weighted speed ($S_{u,L}$) by the relationship $\rho_L S_L = \rho_u S_{u,L}$, with ρ_L and S_L being the local density and speed on the contour and ρ_u being the density of the corresponding unburned fresh mixture. In this paper, the temperature contour of T = 300 K was selected.

Fig. 10 shows the obtained density-weighted flame propagation speed ($S_{u,L}$) versus the local mixture fraction, together with the flame propagation speed of the corresponding 1-D planar premixed flame. The latter was obtained from the web site of GRI Mech 3.0 [19]. It is noted that for the lean and very rich mixture, the local flame speed in the triple flame is higher than that for the 1-D planar flame. However the speed of the 1-D planar flame is higher for the mixture that is rich but close to stoichiometric composition (ξ_s=0.0548). This characteristic is attributed to the effects of flame stretch and heat transfer from the diffusion flame to premixed flame.

The stretch exerts different effects on the flame speeds of rich and lean methane/air mixtures. For lean methane/air mixture, the Lewis number is less than unity. Therefore the stretch increases the flame intensity. For rich methane/air mixture, the stretch reduces the flame intensity due to the Lewis number greater than unity [23]. On the other hand, the heat transfer from the diffusion flame to the premixed flames always enhances the flame speeds. Therefore the effects of both stretch and heat transfer from the diffusion flame cause the local flame speed of the triple flame on the lean side to be higher than the corresponding 1-D planar flame speed. For the very rich mixture of the triple flame, the effect of heat transfer from the diffusion flame is stronger than that of the stretch, and thus the local flame speed of the triple flame is higher than that of the 1-D planar flame. When the mixture is rich but close to the stoichiometric composition, the effect of the stretch exceeds the effect of the heat transfer from the diffusion flame, which causes the higher speed of the corresponding 1-D planar flame.

It can be concluded that both the stretch and the interaction of the diffusion and premixed flames play important roles for the structure and local flame propagation of triple flame.

CONCLUSIONS

The flame in a methane/air mixing layer has been numerically investigated. The results indicate that a triple flame is formed in a methane/air mixing layer. The heat release rate in the diffusion flame is about two orders of magnitude smaller than those in the premixed flames. No fuel can reach the diffusion flame, while oxygen can survive through the lean premixed flame and diffuse to the diffusion flame from lean side. The concentrations of CO_2, H_2O and OH in the diffusion flame are higher than those in premixed flames, while the concentrations of O and H respectively have higher values in lean and rich premixed flames. A triple flame can be stabilized for a flow speed higher than the planar laminar flame speed of a stoichiometric mixture, because of the divergence of streamlines ahead of the flame. The stretch and the interaction of the flame branches play important roles for the structure and local flame propagation for triple flame.

REFERENCES

1. Phillips, H., 10th Symposium (International) on Combustion, The Combustion Institute, Pittsburgh, 1965, pp. 1277-1283.
2. Liñán, A., and Crespo, A., Combust. Sci. Technol. 14:95-117 (1976).
3. Dold, J.W., Combust. Flame 76:71-88 (1989).
4. Kĩoni, P.N., Rogg, B., Bray, K.N.C., and Liñán, A., Combust. Flame 94:276-290 (1993).
5. Ruetsch, G.R., Vervisch, L., and Liñán, A., Phys. Fluids 7: 1447-1454 (1995).

6. Echekki, T. and Chen, J.H., Combust. Flame 114:231-245 (1998).
7. Azzoni, R., Ratti, S., Puri, I.K., and Aggarwal, S.K., Phys. Fluids 11: 3449-3464 (1999).
8. Plessing, T., Terhoeven, P., Peters, N., and Mansour, M.S., Combust. Flame 115:335-353 (1998).
9. Qin, X., Puri, I.K., and Aggarwal, S.K., Proc. Comb. Inst. 29: paper 3D03 (2002).
10. Kĩoni, P.N., Bray, K.N.C., Greenhalgh, and Rogg, B., Combust. Flame 116: 192-206 (1999).
11. Im, H.G., and Chen, J.H., Combust. Flame 119:436-454 (1999).
12. Im, H.G., and Chen, J.H., Combust. Flame 126: 1384-1392 (2001).
13. Lockett, R.D., Boulanger, B., Harding, S.C., and Greenhalgh, D.A.,Combust. Flame 119:109-120 (1999).
14. Kuo, K.K. (1986), Principles of Combustion, John Wiley & Sons.
15. Liu, F., Smallwood, G. J., and Gülder, Ö.L., J. Thermophys Heat Transfer 14:278-281 (2000).
16. Kee., R.J., Dixon-Lewis, G., Warnatz, J., Coltrin, M.E., and Miller, J.A. (1986) "A Fortran computer code package for the evaluation of gas-phase, multicomponent transport properties", Sandia Report, SAND 86-8246.
17. Patankar, S.V. (1980), Numerical Heat Transfer and Fluid Flow, Hemisphere, New York.
18. Liu, Z., Liao, C., Liu, C. and McCormick, S. (1995) "Multigrid method for multi-step finite rate combustion", AIAA 95-0205.
19. Smith, G.P., Golden, D.M., Frenklach, M., Moriarty, N.W., Eiteneer, B., Goldenberg, M., Bowman,C.T., Hanson, R.K., Song, S., Gardiner, W.C., Lissianski, J.V.V., and Qin, Z. (1999) http://www.me.berkeley.edu/gri_mech/.
20. Kee., R.J., Miller, J.A., and Jefferson, T.H. (1980) "A general-purpose, problem-independent, transportable, Fortran chemical kinetics code package", Sandia Report, SAND 80-8003.
21. Bilger, R.W., Twenty-Second Symposium (Int.) on Combustion, The Combustion Institute, Pittsburgh, 1988, pp. 475-488.
22. Glassman, I., Combustion (3rd edition), Academic Press, San Diego, 1996.
23. Law, C.K., and Sun, C.J., Prog. Energy Combust. Sci. 26:459-505 (2000).

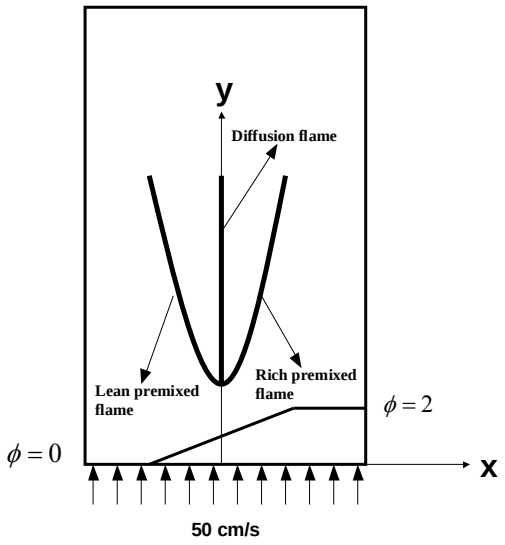

Fig. 1 Flame Configuration

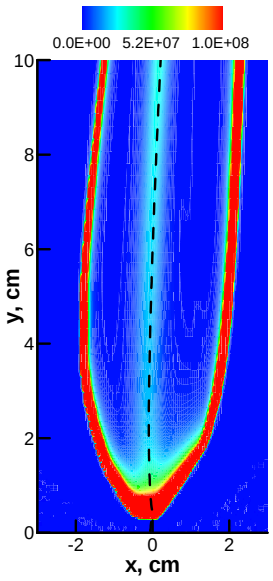

Fig. 2 Distribution of heat release rates.

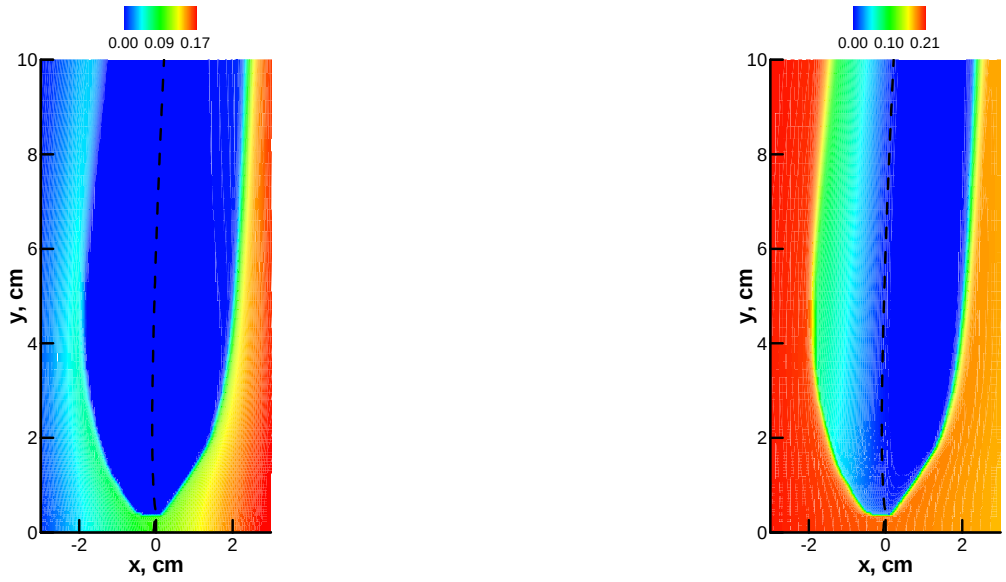

CH_4 O_2

Fig. 3 Mole fractions of fuel (CH_4) and oxygen (O_2).

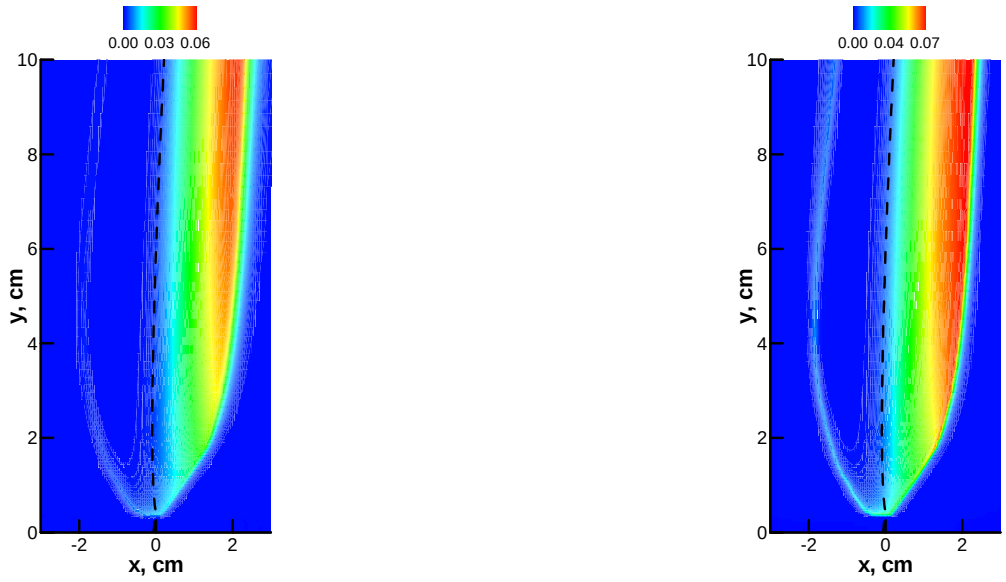

H_2 CO

Fig. 4 Mole fractions of H_2 and CO.

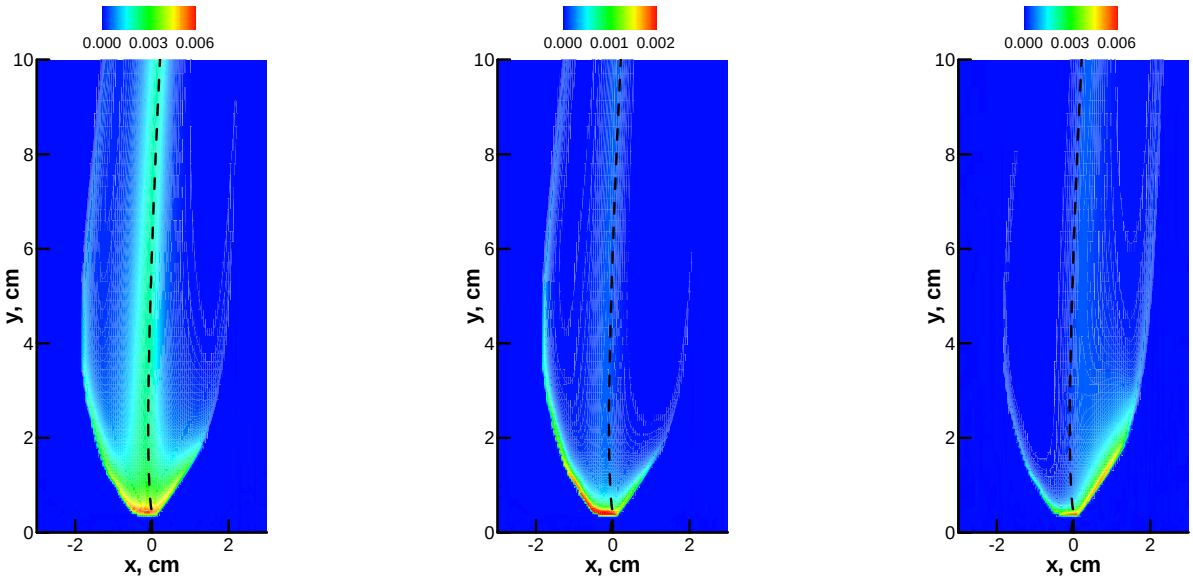

Fig. 5 Mole fractions of OH, O and H.

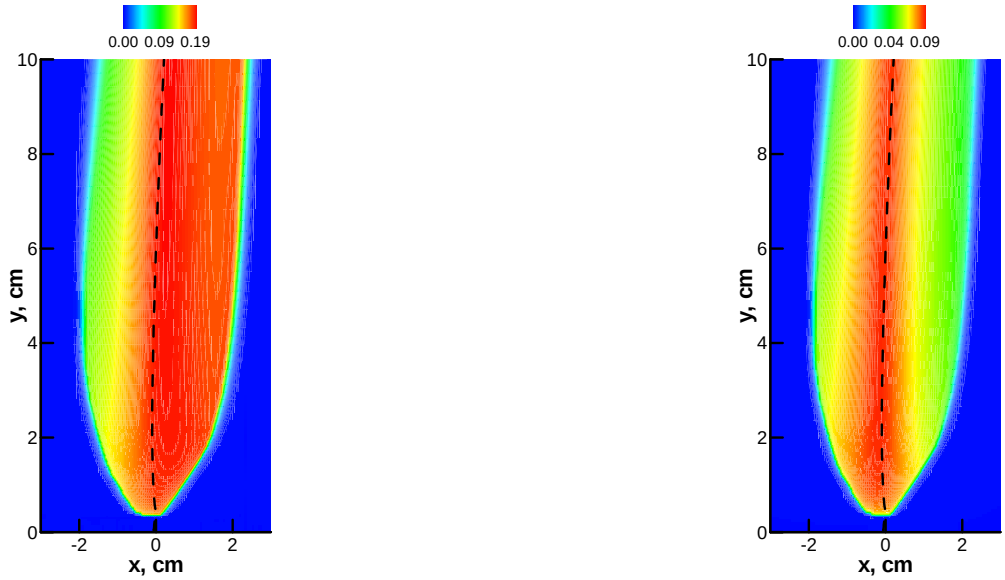

Fig. 6 Mole fractions of H_2O and CO_2.

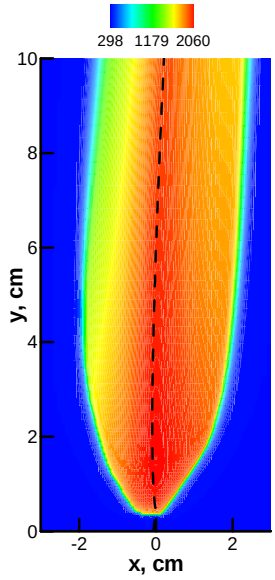

Fig. 7 Temperature distribution, K.

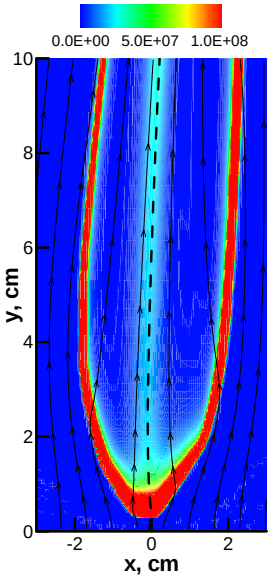

Fig. 8 Streamlines.

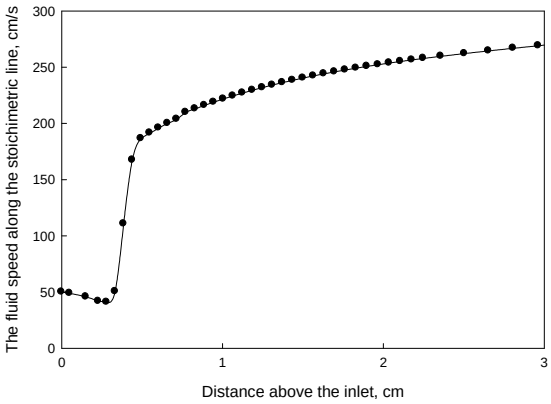

Fig. 9 Fluid speed along the stoichimetric line.

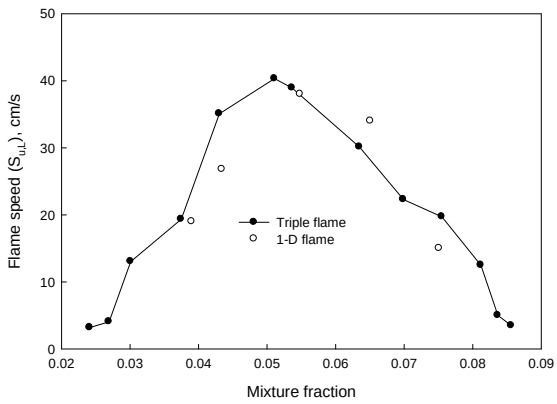

Fig. 10 Local flame propagation speed.